Application of static models to predict midazolam clinical interactions in the presence of single or multiple HCV drugs

Yaofeng Cheng, Li Ma, Shu-Ying Chang, W. Griffith Humphreys and Wenying Li

Pharmaceutical Candidate Optimization, Research and Development, Bristol-Myers Squibb, Princeton,

NJ 08543

1

DMD #70409

Running Title: Predicting CYP3A4-mdeiated DDI risk for HCV drug combination

Corresponding Author: Dr. Wenying Li,

Pharmaceutical Candidate Optimization,

Bristol-Myers Squibb, P.O. Box 4000,

Princeton, NJ 08543,

Email: Wenying.Li@BMS.com.

Number of text pages = 24

Number of tables = 5

Number of figures = 3

Number of references = 37

Number of words in the abstract = 248

Number of words in the introduction = 734

Number of words in the discussion = 1760

Abbreviations: ASV, Asunaprevir; DCV, daclatasvir; BCV, beclabuvir; TDI, time dependent inhibition; DDI, drug-drug interactions; CYP, cytochrome P450; NCE, new chemical entity; PXR, pregnane X receptor; CAR, constitutive androstane receptor; AhR, aryl hydrocarbon receptor; HCV, hepatitis C virus; LDH, lactate dehydrogenase; GAPDH, Glyceraldehyde 3-phosphate dehydrogenase.

Abstract

Asunaprevir (ASV), daclatasvir (DCV), and beclabuvir (BCV) are three drugs developed for the treatment of chronic hepatitis C virus infection. Here we evaluated the CYP3A4 induction potential of each drug, as well as BCV-M1 (the major metabolite of BCV), in human hepatocytes by measuring CYP3A4 mRNA alteration. The induction responses were quantified as Induction Fold (mRNA fold change) and Induction Increase (mRNA fold increase), and then fitted with 4 non-linear regression algorithms. Reversible inhibition and time dependent inhibition (TDI) on CYP3A4 activity were determined in order to predict net drug-drug interactions (DDI). All four compounds were CYP3A4 inducers and inhibitors, with ASV demonstrating TDI. The curve fitting results demonstrated that Fold Increase is a better assessment to determine kinetic parameters for compounds inducing weak responses. By summing the contribution of each inducer, the basic static model was able to correctly predict the potential for a clinically meaningful induction signal for single or multiple perpetrators, but with over prediction of the magnitude. With the same approach, the mechanistic static model improved the prediction accuracy of DCV and BCV when including both induction and inhibition effects, but incorrectly predicted the net DDI effects for ASV alone or triple combinations. The predictions of ASV or the triple combination could be improved by only including the induction and reversible inhibition but not the ASV CYP3A4 TDI component. Those results demonstrated that static models can be applied as a tool to help project the DDI risk of multiple perpetrators using in vitro data.

INTRODUCTION

The study of cytochrome P450 (CYP) enzyme induction has important clinical significance for drug development. According to the US Food and Drug Administration (FDA) guidance for industry, one of the major objectives in evaluating *in vitro* drug metabolism is to explore the effects of the new chemical entity (NCE) on the metabolism of other drugs and the effects of other drugs on its metabolism(US-FDA Draft Guidance, 2012). Induction of CYP enzymes may lead to reduced efficacy or adverse drug interactions by increasing the metabolism of other drugs that are substrates for the induced enzymes (Jana and Paliwal, 2007). Therefore, it is important to determine whether a drug candidate has the potential to interact with CYP enzymes. If this determination can be made in discovery or early development, the data can aid in more efficient clinical trial design. In addition, a negative result from *in vitro* experiments may preclude or reduce the need to perform corresponding *in vivo* clinical drug interaction studies.

Human microsomes are commonly used to investigate the inhibitory effect of drug candidates in vitro since the CYP activities are well maintained in those systems. However, CYP induction is mainly through the bindings of drugs to nuclear receptors that then guide the protein expression of a specific enzyme. For example, the induction of CYP3A4, CYP2B6, and CYP1A1 are through the activation of upstream transcription factors including pregnane X receptor (PXR), constitutive androstane receptor (CAR), and aryl hydrocarbon receptor (AhR) (Tompkins and Wallace, 2007). Therefore, the in vitro induction experiments are usually conducted in living cells, mostly in hepatocytes. Evaluation of CYP1A2, CYP2B6, and CYP3A mRNA induction in primary human hepatocytes are recommended with the generation of E_{max} and EC_{50} values, which can then be used in model-based analysis to determine the potential for an in vivo signal and the need for further clinical evaluation.

Asunaprevir (ASV, BMS-650032), daclatasvir (DCV, BMS-790052), and beclabuvir (BCV, BMS-791325) are three drugs developed for chronic hepatitis C virus (HCV) infection. ASV is a potent

and selective inhibitor of HCV NS3 protease, with activity against genotypes 1 and 4 (McPhee et al., 2012). DCV is a highly selective HCV NS5A replication complex inhibitor with picomolar potency and antiviral activity against HCV genotypes 1-6 *in vitro* (Gao et al., 2010). BCV is a selective, nonnucleoside NS5B polymerase inhibitor (Gentles et al., 2014). These new generation HCV drugs have less complications when comparing with conventional treatments consisting of a combination of antiviral drug(s) (i.e. ribavirin) and pegylated interferon (Wilkins et al., 2010). DCV and ASV dual regimen has been approved in Japan and several nations across Asia Pacific, Latin America, and Eastern Europe for patients with genotype 1 chronic HCV infection and DCV has been approved in in US, Europe, Japan, and multiple nations across Latin America, Middle East and Asia Pacific for use in combination with other medicines for HCV genotypes 1, 2, 3 and 4. The triple combination of DCV, ASV and BCV is under regulatory review.

Following an oral dose, metabolites contribute less than 10% of the drug related systemic exposure in human for both ASV and DCV (Gong et al., 2015; Eley et al., 2013). A major metabolite of BCV, BCV-M1, was observed in human, up to 24.6% of total exposure in plasma (Sims et al., 2014). Based on FDA draft guidance (US FDA 2008), metabolites found at greater than 10 percent of parent drug systemic exposure at steady state in human plasma can raise a safety concern and should be characterized. The 10 percent threshold was further clarified and a major metabolite is defined as a human metabolite that comprises greater than 10 percent of the measured total exposure to drug and metabolites (US FDA 2013). Therefore, BCV-M1, but no other metabolite of these HCV drugs, was characterized in non-clinical studies, including in vitro CYP inhibition and induction evaluations. Since inhibition assays were conducted following the well-established methods (Yao et. al., 2007; Chang et. al 2010) with minor changes, results of those studies are presented without inclusion of experimental methods. Here, we describe our experience and rationale for conduction of induction studies, including experiment design, selection of data sets and non-linear regression algorithms for curve fitting to

determine induction E_{max} and EC_{50} values, and provide a structured approach for data processing. In addition, we explored the possibility using basic and mechanistic static models to predict the in vivo DDI risk in the presence of multiple perpetrators.

MATERIALS AND METHODS

Chemicals

Asunaprevir (ASV, BMS-650032), daclatasvir (DCV, BMS-790052), and beclabuvir (BCV, BMS-791325) and BCV-M1 (a major metabolite of BCV) were synthesized at Bristol-Myers Squibb Co (New Brunswick, NJ) (Scola et al., 2014; Gao et al., 2010; Gentles et al., 2014). Their structures are shown in Figure 1. Rifampin was purchased from Sigma (St. Louis, MS). All other reagents and solvents were of analytical grade.

CYP3A4 induction in human hepatocytes

The criteria to select compound concentrations were based on the clinical maximum plasma concentration (C_{max}) at steady state and the highest concentration which did not cause cytotoxicity evaluated by LDH release. Concentrations of each test compound were: ASV (0.049, 0.15, 0.49, 1, 2, 4.9, 10 and 20 µg/mL), DCV (0.16, 0.32, 0.75, 1.6, 2.5, 4, 6 and 9.6 µg/mL), BCV (0.15, 0.35, 0.8, 1.5, 3.5, 8, 15 and 30 µg/mL) and BCV-M1 (0.028, 0.08, 0.28, 0.8, 2.8, 8, 15, and 30 µg/mL). The CYP induction experiments were conducted by XenoTech LLC (Lenexa, KS), using sandwich cultured cryopreserved hepatocytes from 3 male donors, according to XenoTech's protocol and previously described methods (Madan et al., 2003; Paris et al., 2009; Robertson et al., 2000). Each compound was tested with 3 different lots of hepatocytes. Hepatocyte Lot HC3-15, Lot HC5-10, and Lot HC1-18 were used to evaluate ASV and DCV, while hepatocyte Lot HC3-15, Lot HC5-10, and Lot HC3-17 were used for BCV and BCV-M1. The hepatocyte cultures were treated for 3 consecutive days with 0.1% v/v DMSO (vehicle control), BMS compounds, or rifampin (10 µM, positive control). Cytotoxicity was assessed by visual inspection of cell morphology and by measuring lactate dehydrogenase (LDH) activity in the incubation media with the Cytotoxicity Detection Kit (Roche Diagnostics Co., Indianapolis, IN). Approximately 24 hours following the last treatment, media was removed. The cells were washed with fresh culture media and total RNA was isolated from the cells using TRIzol RNA

DMD #70409

Isolation Reagent (Life Technologies, Grand Island, NY) and purified using the RNAeasy Mini Kit (Qiagen Inc. Gaithsburg, MD), according to manufacturers' instructions. Single-stranded cDNA preparation and quantitative RT-PCR were performed using the AB 7900HT Fast Real Time PCR System (Applied Biosystems, Foster City, CA) following the Applied Biosystem protocol. qRT-PCR data were processed using the Sequence Detection System (SDS) Software Version 1.4 or 2.3, for Relative Quantification (Applied Biosystems). Target gene (CYP3A4) signals are normalized to the endogenous gene control (GAPDH) as $\Delta C_t = C_t$ (CYP3A4) $- C_t$ (GAPDH). Relative gene expression was obtained by comparing normalized target gene signal in compound treated sample to vehicle control $(2^{-[\Delta C_t(\text{test compound}) - \Delta C_t(\text{vehicle control})]})$, which is defined as Fold Induction in this manuscript. Fold Increase is the change of gene expression which is calculated as follows: Fold Increase = Fold Induction -1.

In vitro induction model fitting

The maximum induction response (E_{max}) and concentration causing half Emax (EC_{50}) were calculated based on both Fold Induction and Fold Increase data. For the purpose of curve fitting, data points were excluded from the fitting if they had concentrations greater than the one causing the highest response (observed E_{max}) but had measured mRNA level less than 80% of the observed E_{max}. Induction response were fit using the following four non-linear regression algorithms (model) using GraphPad Prism Version 5 (GraphPad Software, Inc., La Jolla, CA) or Sigma Plot V12 (Systat Software, Inc., San Jose, CA):

$$\text{Simple } E_{max} \text{ Model:} \quad E = \frac{\text{Emax} \times C}{EC50 + C} \qquad (1)$$

$$\text{Sigmoid Hill Model:} \quad E = \frac{\text{Emax} \times C^H}{EC50^H + C^H} \qquad (2)$$

$$\text{Sigmoid 3 Parameter Model:} \quad E = \frac{\text{Emax}}{1 + e^{(EC50 - C)/H}} \qquad (3)$$

$$\text{Four Parameter Logic Model:} \quad E = D + \frac{\text{Emax} - D}{1 + (\frac{EC50}{C})^H} \qquad (4)$$

8

DMD #70409

In which E is the observed induction effect in the presence of inducer at different concentration (C), and

D in Equation 4 stands for the induction effect after the treatment with DMSO vehicle.

The best fit model was selected based on the lowest Corrected Akaike's information criterions (AICc),

which were calculated as the following equation:

$$AICc = N \times \ln \frac{SS}{N} + \frac{2N \times P}{N - P - 1} \tag{5}$$

where N is the number of data points used in the fitting, SS is the residual sum of squares of the fitting,

and P is the number of parameters in the fitting model (Sugiura, 1978).

CYP3A4 inhibition assays in human liver microsomes

To predict the net DDI effect, the reversal inhibition and time dependent inhibition of ASV,

DCV, BCV and BCV-M1 on CYP3A4 were evaluated in human liver microsomes based on published

methods (Yao et. al., 2007; Chang et. al 2010). A brief description of experiment procedures and data

processing is available in the Supplemental Information (Supplemental Methods). Concentration of

midazolam in the assay (5 μM) was close to the K_M value of midazolam determined in the assay (4.13

μM) (Yao et al., 2007), therefore Ki value was estimated to be 1/2 of IC50 value according to the

Cheng-Prusoff equation (Chen et al., 1972) by assuming that the test compound is a competitive

inhibitor of CYP3A4 midazolam 1'-hydroxylation activity. All incubations were run in triplicate and the

mean values of the triplicates were used for calculation of the inhibition parameters.

In vivo interaction prediction

The in vivo DDI risk was predicted using modified basic static model (R3) and mechanistic

static model (AUCR), as described below.

$$R3 = \frac{1}{1 + \sum_{p=1}^{n} \frac{d * E_{\max,p} \times [I]_p}{[I]_p + EC_{50,p}}} \tag{6}$$

$$AUCR = \frac{1}{f_m \times (A \times B \times C) + (1 - f_m)} \times \frac{1}{(X \times Y \times Z) \times (1 - F_G) + F_G} \tag{7}$$

9

DMD #70409

In which A, B, and C represent the reversible inhibition, time dependent inhibition (TDI) and induction in liver, respectively, and X, Y, and Z represent the reversible inhibition, TDI and induction in GI track. They were defined as shown below

$$A = \frac{1}{1 + \sum_{p=1}^{n} \frac{[I]_{H,p}}{K_{i,u,p}}} \tag{7.1}$$

$$B = \frac{k_{deg,H}}{k_{deg,H} + \sum_{p=1}^{n} \frac{[I]_{H,p} \times k_{inact,p}}{[I]_{H,p} + K_{I,u,p}}} \tag{7.2}$$

$$C = 1 + \sum_{p=1}^{n} \frac{d \times E_{max,p} \times [I]_{H,p}}{[I]_{H,p} + EC_{50,p}} \tag{7.3}$$

$$X = \frac{1}{1 + \sum_{p=1}^{n} \frac{[I]_{G,p}}{K_{i,u,p}}} \tag{7.4}$$

$$Y = \frac{k_{deg,G}}{k_{deg,G} + \sum_{p=1}^{n} \frac{[I]_{G,p} \times k_{inact,p}}{[I]_{G,p} + K_{I,u,p}}} \tag{7.5}$$

$$Z = 1 + \sum_{p=1}^{n} \frac{d \times E_{max,p} \times [I]_{G,p}}{[I]_{G,p} + EC_{50,p}} \tag{7.6}$$

p is the number of perpetrators. $[I]$ in Equation 6 is the total plasma concentration. The degradation rates for CYP3A4 in the liver ($k_{deg,H}$) and intestine ($k_{deg,G}$) were 0.00032 and 0.00048/min, (Fahmi et al., 2009; Fahmi et al., 2008). The fraction of the midazolam metabolized by CYP3A (f_m) and the fraction of midazolam escaping intestinal extraction (F_G) are 0.90 and 0.51, respectively (Obach et al., 2007). $K_{i,u}$, K_{inact} and $K_{I,u}$ represent the unbound reverse inhibition constant, maximum inactivation (K_{inact}) and TDI constant, respectively. d represents a calibrator factor and a value of 1 is used for both Equitation 6 and 7. $[I]_H$ and $[I]_G$ in Equation 7.1-7.6 represent the perpetrator free portal vein concentration and gut enterocytes concentration, respectively, which are estimated:

$$[I]_H = f_u \times (C_{max} + \frac{D \times Ka \times Fa}{Q_H \times BP}) \tag{7.7}$$

$$[I]_G = \frac{D \times Ka \times Fa}{Q_G} \tag{7.8}$$

10

D is the oral dose and f_u is the fraction of unbound drug in human serum. The values of hepatic blood flow (Q_H) and enterocytes blood flow (Q_G) used here are 1616 mL/min and 300 mL/min, respectively. The first order absorption rate (Ka) was determined by first order modeling fitting of plasma concentration profile following an oral dose using Phoenix WinNonlin. The human blood-to-plasma ratio (BP) for DCV, ASV and BCV were determined to be 0.8, 0.55, and 0.7, respectively (unpublished data). Fraction of absorption (Fa) was derived from absolute bioavailability (F) and fraction of dose that escapes first pass metabolism in gut (Fg) and liver (Fh) using the equation F=Fa × Fg × Fh, in which Fg was assumed to be 1. As hepatic clearance is the major clearance pathway for DCV (DAKLINZA[TM] package insert, 2016), ASV (SUNVEPRA[®] package insert, 2015), as well as BCV (unpublished data), Fh can be estimated based on Fh = 1-CL/(bp × Q_H), in which CL is the plasma clearance and bp is blood-to-plasma ratio. F and CL values were obtained in clinical studies as 67% and 4.2 L/h for DCV (DAKLINZA[TM] package insert, 2016), 9.3% and 49.5 L/h for ASV (SUNVEPRA[®] package insert, 2015), and 66.1% and 5.6 L/h for BCV (unpublished data).

To predict the *in vivo* induction effect in the presence of single perpetrator, R3 values were calculated using either the average or individual values of EC_{50} and E_{max} or individual ones from 3 different donors. In the case of AUCR, the net DDI effects of ASV, DCV and BCV were determined with average inhibitor kinetic parameters together with average or individual EC_{50} and E_{max}. Since only two lots of hepatocytes (Lot HC3-15 and Lot HC5-10) were used to test the induction potential of all 4 compounds, the individual R3 and AUCR for combination treatments were only calculated in those two cases.

DMD #70409

Results

The CYP3A4 mRNA induction data for ASV, DCV, BCV and BCV-M1 are listed in Table 1. The positive control of CYP3A4 inducer, rifampin, caused 3.7 to 29.8 fold induction compared with DMSO vehicle control in three human donors, suggesting that the assay system functioned with adequate sensitivity. Upon treatment of cryopreserved human hepatocytes with test compounds, bell-shaped induction-concentration curves were observed for ASV, BCV and BCV-M1. This may be caused by mild cytotoxicity effects at higher concentrations, even though it was not evidenced in the LDH release assay.

The induction response was fitted to four kinetic models as described in the Methods section. E_{max} and EC_{50} values of each compound fitting using all four models are presented in Supplemental Table 2. AICc values were calculated for each model and the model with the lowest AICc value was selected to determine induction kinetic parameters. Among the 24 model fittings, the Simple E_{max} Model was selected most frequently (15/24). The determined E_{max} and EC_{50} values are summarized in Table 2. BCV was the most potent inducer among the four compounds followed by BCV-M1, ASV and DCV.

For comparison, both Fold Induction and Fold Increase of mRNA levels were fitted with the four kinetic models. Different outcomes with Fold Induction and Fold Increase were observed (Table 2). The differences may not be noticeable in the results with large induction response, but become significant with small induction response (up to 15 fold difference between Fold Induction and Fold Increase). As an example, curve fitting with the Simple E_{max} Model gave quite different EC_{50} values for Fold Induction and Fold Increase (Figure 2). The difference was most significant for Donor 2 with whom the observed E_{max} was small (Figure 2-C). While applying Four Parameter Logic Model, EC_{50} were not different when fitting with Fold Induction and Fold Increase (Figure 2- D). However, since Four Parameter Logic Model generated a larger AICc value, it was not selected for E_{max} and EC_{50}

DMD #70409

determination. With the corrected induction response (Fold Increase), an EC_{50} value of 0.45 µg/mL was determined as shown in Figure 2-C and it is very close the value (EC_{50}: 0.36 µg/mL) from Figure 2-D.

DCV, ASV, BCV and BCV-M1 were also found to be inhibitors of CYP3A4 in human liver microsome incubations. The initial study found that the four drugs demonstrated increased potency to inhibit CYP3A4 with 30 min pre-incubation (Supplemental Figure 1 and Supplemental Table 1). The IC_{50} values of DCV, BCV and BCV-M1 was reduced approximately by half, but the IC_{50} of ASV was decreased more than 5 fold. Thus, the TDI of ASV was further evaluated to determine TDI kinetics (Supplemental Figures 2, Supplemental Figure 3, and Supplemental Table 1). The parameters for DDI predictions are listed in Table 3.

Several clinical studies have been conducted to evaluate the effects of HCV drugs at different doses and combinations on the pharmacokinetics of midazolam. The study design, doses, and observed pharmacokinetic parameters are summarized in Table 4. The in vivo interaction effects were first estimated using the basic static model (R3). In the treatment of ASV (200 and 600 mg) or DCV (60 mg), a single inducer was considered in the prediction. In the treatment of BCV (150 and 300 mg), Triple I or Triple II, R3 values were calculated based the effect of multiple inducers. Overall, R3 can correctly predict the in vivo induction risk, in both cases using either average or individual E_{max} and EC_{50}. All the seven treatments were predicted to cause induction effect, which agree with the clinical results (Table 5). However, R3 over predicted the induction potency for both single inducer and multiple inducers.

The "net DDI effect" of these perpetrators on midazolam exposure was also estimated using the mechanistic static model. When considering the induction together with inhibition, the mechanistic static model were able to correctly predict the interaction risk of DCV (60 mg QD) and BCV (150 mg BID and 300 mg BID). As shown in Table 5, the predicted AUC ratios (AUCR) using average E_{max} and EC_{50} values are 0.43, 0.53, and 0.55 for the group of DCV (60 mg QD), BCV (150 mg BID) and BCV (300 mg BID), respectively. Additionally, the AUCR values are closer to the observed clinical AUC changes

13

than the R3 values. However, mechanistic static model predicted net inhibition (AUCR>1) for the clinical studies with ASV and two triple combinations while considering induction, inhibition and TDI. Those false predictions were corrected by not including the TDI component of ASV on CYP3A4 activity. This adjusted mechanistic static model (AUCR') not only could predict the induction risk for ASV and triple combinations but also returned a better results than the basic static model (R3). Similar results were also observed when using the individual E_{max} and EC_{50} values to predict net DDI effect.

Discussion

Hepatocytes are widely recognized as the most appropriate in vitro model to study the potential of new drugs to induce hepatic metabolism enzymes. Due to interspecies differences, primary cultures of human hepatocytes have become the system of choice over studies performed in animals. It has been shown that when human hepatocytes are overlaid with extracellular matrix, such as Matrigel® or collagen, the cells retain the ability to respond to prototypical cytochrome P450 inducers (LeCluyse et al., 2000; LeCluyse, 2001). This straightforward screening method has been of great importance to drug development efforts, yielding both predictive and species-relevant data. To best determine the values of E_{max} and EC_{50} in human hepatocytes, 6 to 8 concentrations of the test compound are recommended. In general, the lowest test concentration should be set close to 1/10th of the maximum plasma concentration (or projected maximum plasma concentration) in humans at a relevant clinical dose, while the top test concentration should go as high as possible to reach the induction response plateau, unless the response is limited by solubility or cytotoxicity. Despite the general consensus on basic experimental design there remains some inconsistencies in data processing methods and a general lack of results on how to extrapolate in vitro induction data on single compounds to clinical situations involving mixtures of those compounds.

Four non-linear regression algorithms, Simple E_{max}, Sigmoid Hill, Sigmoid 3 Parameter and Four Parameter Logic model, have been suggested for curve fitting of in vitro induction data (Einolf et al., 2014). Induction studies often are designed with the number of test concentration levels set as to collect a robust data set (as mentioned above, 8 concentrations), but also conserve the number of hepatocytes used. The number of data points may become even smaller in the case of solubility or cytotoxicity issues and for many compounds these factors can provide challenges to getting complete response values over the concentration range of interest. For the four compounds tested in our study, three seemed to cause mild cytotoxicity, evidenced by the decreased induction at higher concentration, however, the

cytotoxicity was not detected via be measured by LDH release assay. These data points were excluded

from the analysis and thus the experiment produced a reduced number of data points for regression

models. A model with higher number of parameters tends to over-fit the induction data as it has more

freedom to fit. Thus, AICc value can be used to compare models and select the best fit one since it

corrects sample size and is considered more accurate with small sample size (Sugiura, 1978). If $N \leq P$,

the model should not be considered as it indicated that there are insufficient data points. If $N = P+1$,

AICc will not be calculable, but the model can be selected if other models fail. In addition, different

from using standard error or R-squares as a way to select the best fit model, AICc method penalizes

extra parameters (P) for a fitting model. Not surprisingly, with 4 to 7 available data points in our

induction data set, Simple E_{max} model was selected in most of the cases to be the best fit model over the

other three models.

An aspect of data processing to determine induction parameters that is not entirely consistent in

the literature is how to fit the "no induction" value when performing curve fitting. The value of Fold

Induction has been used to calculate E_{max} and EC_{50} values in many literature reports. The Fold Induction

parameter would normally be set at "1" for the vehicle control. However, for the Simple E_{max} and

Sigmoid Hill models the values should more appropriately be set at "0". To correct this discrepancy, we

have used a parameter termed Fold Increase (as defined in the Methods section). While fitting with the

Fold Induction value, the under estimation of EC_{50} values may not be noticeable for compounds with

large induction responses, it can be significant for compounds with low induction response, as shown in

Figure 2. In addition, the E_{max} determined using Fold Increase is more consistent with results from

induction prediction models. For example, the E_{max} values for a non-inducer based on Fold Increase

would be "0" and thus the calculated induction effect ($R3 = 1/(1 + E_{max}*[I]/(EC_{50} + [I]))$) would be 1 (no

induction effect). Overall, Fold Increase is a more appropriate parameter for curve fitting to generate

induction parameters.

The basic static model (R3) is a simplified model to predict in vivo DDI risk which only

considers the induction potential of the perpetrator (E_{max} and EC_{50}) at maximum plasma concentration.

Therefore, R3 tends to over-predict induction effects. This is apparent in our predictions from all seven

clinical DDI studies, in which R3 values were lower in each case than the observed AUC ratios.

However, R3 did correctly predict an induction response as defined as R3<0.9 in these seven treatments

with either single or multiple perpetrators. The mechanistic static model is a more complicated model to

evaluate the "net effect" of a perpetrator which demonstrates induction, inhibition and inactivation

simultaneously in both liver and small intestine. This model also considers the characteristics of victim

drugs, such as absorption and fractional metabolism through the pathway of interest. In the seven cases,

the mechanistic static model was able to correctly predict the interaction risk of DCV (60 mg QD) and

BCV (150 mg BID and 300 mg BID). Since the reversible inhibition effect was considered in this

model, the predicted values are closer to the clinical observations than the R3 values. When the TDI

effect of ASV was included, the mechanistic static model incorrectly predicted the DDI risk of ASV

(200 mg BID and 600 mg BID). This false prediction could be corrected by not including the

inactivation component (B and Y in Equation 7), as shown in Table 4, which was also reported

previously by Einolf et al. (Einolf et al., 2014). The detailed mechanisms for the over-prediction of ASV

TDI remain unclear. One of the explanations could be that the rapid clearance of ASV minimizes its

long-last inactivation effect on CYP3A4, therefore a reduced overall inhibition in vivo. The first pass

plasma metabolic clearance of ASV was found 49.5 L/h in the clinic (SUNVEPRA® package insert,

2015). This has been observed for other high clearance drugs which demonstrated potent in vitro TDI

but lower than projected clinic DDI, such as raloxifene and ezetimibe (Zientek and Dalvie, 2012;

Parkinson et al., 2010; Kosoglou et al., 2005). Based on these results, it seems that there is a need for

17

better treatments of inducers that are also TDIs and the prediction of the net DDI effect of a drug which

demonstrates both induction and inactivation effect should be carefully considered. In this study, we also

compared the model predictions applying either average induction parameters (EC_{50} and E_{max}) or

individual values. The predicted DDI using individual parameters can potentially provide a range of

ratios which could represent the individual viability in clinic. However, the small number of hepatocyte

lots that are typically studied in vitro makes it very difficult to derive a meaningful projection of inter-

individual variability and likely does not provide useful information.

Many models have been developed to extrapolate *in vitro* results to *in vivo* observations,

including static and dynamic models, in which physiologically based pharmacokinetic (PBPK) modeling

is widely applied to predict in vivo DDI. However, to date PBPK-based approaches have been limited to

prediction of DDI with one perpetrator and it is very challenging to predict the DDI risk of mixtures of

drugs using PBPK modeling software. Here we explored the possibility to predict DDI with multiple

inducers using static models. It has been reported that the total inhibition of multiple competitive

inhibitors can be projected using the summed inhibition of each inhibitor (Lutz and Isoherranen, 2012;

Venkatakrishnan et al., 2003). In this study, we assumed that the four compounds induced CYP3A4

enzymes all through the PXR receptor, since no CYP2B6 and CYP1A2 induction was observed in the

hepatocyte experiment (data not shown). Therefore, the total induction was estimated using the summed

induction of each compound, as described in Equation 6 and 7. With these approaches, we were able to

predict the net DDI risk in the presence of multiple perpetrators. Inclusion of TDI overpredicted the DDI

risk for ASV alone, which then led to over prediction for two triple combination treatments including

ASV. However, improved prediction was achieved for ASV when not including the TDI component.

Therefore, applying the correct prediction strategy of each single perpetrator, we were able to correctly

predict the DDI risk in the presence of all four perpetrators when coadministered. Based on these

examples, we propose a strategy to evaluate net DDI risk with multiple perpetrators that are inducers

and have a TDI component as shown in Figure 3. If AUCR correctly predicts clinical DDI for single perpetrator, it is suggested to use AUCR for DDI prediction of multiple perpetrators. Otherwise, prediction based on AUCR' should be evaluated, as our results and other literature reports have shown the over prediction when one or more of the drugs has a TDI component (Einolf et al., 2014; Zientek and Dalvie, 2012; Parkinson et al., 2010; Kosoglou et al., 2005). In the case that clinical DDI of each single perpetrator is unknown, we suggest calculation of both AUCR and AUCR' for co-administered drugs, with the use of these values according to safety and efficacy considerations of the victim drugs; prediction with AUCR may be more appropriate with victim drugs that have safety concern for over-exposure, while prediction with AUCR' may be more appropriate with victim drugs that have efficacy concern for under-exposure.

While experiments using human hepatocytes have been widely accepted as the gold standard to investigate the induction effect of new chemical entities on CYP enzymes, there still remains some questions as exactly how to interpret induction results and translate the in vitro data into in vivo. This is especially true for compounds that display complex inhibition and induction effects or are administered as combinations. In this study, we found that DCV, ASV, BCV and BCV-M1 were inducers of CYP3A4 in human hepatocytes. The induction responses were fit with several models in order to determine kinetic parameters, and AICc criteria were used to select the best regression fitting algorithms. The Fold Induction parameter was replaced by Fold Increase which more accurately determined E_{max} and EC_{50}. This modification is especially important for compounds producing small induction effects. With model optimization and validation for single perpetrator prediction, the basic or mechanistic static model was able to predict the DDI risk for multiple perpetrators based on in vitro results.

DMD #70409

ACKNOWLEDGEMENTS

AUTHORSHIP CONTRIBUTIONS

Participated in research design: Cheng, Li

Conducted experiments: Cheng, Ma, Chang, Li

Performed data analysis: Cheng, Li

Wrote or contributed to the writing of the manuscript: Cheng, Humphreys, Li

DMD #70409

REFERENCES:

AbuTarif M, He B, Ding Y, Sims K, Zhu K, Rege B, Pursely J, Wind-Rotolo M, Li W and Bertz RJ (2014) The Effect of Steady-state BMS-791325, a Non-nucleoside HCV NS5B Polymerase Inhibitor, on the Pharmacokinetics of Midazolam in Healthy Japanese and Caucasian Males, 15th International Workshop on Clinical Pharmacology of HIV and Hepatitis Therapy.

Bifano M, Sevinsky H, Stonier M, Hao J and Bertz RJ (2013) Daclatasvir, an HCV NS5A Replication Complex Inhibitor, Has Minimal Effect on Pharmacokinetics of Midazolam, a Sensitive Probe for Cytochrome P450 3A4, 8th International Workshop on Clinical Pharmacology of Hepatitis Therapy.

Chang SY, Fancher RM, Zhang H, Gan J (2010) Mechanism-based inhibition of human cytochrome P4503A4 by domperidone. Xenobiotica.40:138-145.

Cheng Y, Prusoff WH (1973) Relationship between the inhibition constant (K_I) and the concentration of inhibitor which causes 50 per cent inhibition (I_{50}) of an enzymatic reaction. Biochem Pharmacol **22**: 3099–3108.

DAKLINZA™ [package insert] (2016). Bristol-Myers Squibb, Inc. Princeton, NJ, USA
http://packageinserts.bms.com/pi/pi_daklinza.pdf

Einolf HJ, Chen L, Fahmi OA, Gibson CR, Obach RS, Shebley M, Silva J, Sinz MW, Unadkat JD, Zhang L and Zhao P (2014) Evaluation of various static and dynamic modeling methods to predict clinical CYP3A induction using in vitro CYP3A4 mRNA induction data, Clin Pharmacol Ther **95**:179-188.

Eley T, Gardiner DF, Persson A, He B, You X, Vaishali Shah, Diane Sherman, Hamza Kandoussi, Karen D. Sims, Claudio Pasquinelli and R.J. Bertz (2011) Evaluation of Drug Interaction Potential of the HCV Protease Inhibitor Asunaprevir (ASV; BMS-650032) at 200 mg Twice Daily (BID) in Metabolic Cocktail and P-glycoprotein (P-gp) Probe Studies in Healthy Volunteers, 62th Annual Meeting of the American Association for the Study of Liver Diseases #381.

Eley T, He B, Huang S-P, Li W, Pasquinelli C, Rodrigues AD, Grasela DM and Bertz RJ (2013) Pharmacokinetics of the NS3 Protease Inhibitor, Asunaprevir (ASV, BMS-650032), in Phase I Studies in Subjects With or Without Chronic Hepatitis C, Clinical Pharmacology in Drug Development **2**:316-327.

Fahmi OA, Maurer TS, Kish M, Cardenas E, Boldt S and Nettleton D (2008) A combined model for predicting CYP3A4 clinical net drug-drug interaction based on CYP3A4 inhibition, inactivation, and induction determined in vitro, Drug Metab Dispos **36**:1698-1708.

Fahmi OA, Hurst S, Plowchalk D, Cook J, Guo F, Youdim K, Dickins M, Phipps A, Darekar A, Hyland R and Obach RS (2009) Comparison of different algorithms for predicting clinical drug-drug interactions, based on the use of CYP3A4 in vitro data: predictions of compounds as precipitants of interaction, Drug Metab Dispos **37**:1658-1666.

Gao M, Nettles RE, Belema M, Snyder LB, Nguyen VN, Fridell RA, Serrano-Wu MH, Langley DR, Sun JH, O'Boyle DR II, Lemm JA, Wang C, Knipe JO, Chien C, Colonno RJ, Grasela DM, Meanwell

21

DMD #70409

NA and Hamann LG (2010) Chemical genetics strategy identifies an HCV NS5A inhibitor with a potent clinical effect, Nature **465**:96-100.

Gentles RG, Ding M, Bender JA, Bergstrom CP, Grant-Young K, Hewawasam P, Hudyma T, Martin S, Nickel A, Regueiro-Ren A, Tu Y, Yang Z, Yeung KS, Zheng X, Chao S, Sun JH, Beno BR, Camac DM, Chang CH, Gao M, Morin PE, Sheriff S, Tredup J, Wan J, Witmer MR, Xie D, Hanumegowda U, Knipe J, Mosure K, Santone KS, Parker DD, Zhuo X, Lemm J, Liu M, Pelosi L, Rigat K, Voss S, Wang Y, Wang YK, Colonno RJ, Gao M, Roberts SB, Gao Q, Ng A, Meanwell NA and Kadow JF(2014) Discovery and preclinical characterization of the cyclopropylindolobenzazepine BMS-791325, a potent allosteric inhibitor of the hepatitis C virus NS5B polymerase, J Med Chem **57**:1855-1879.

Gong J, Eley T, He B, Arora V, Philip T, Jiang H, Easter J, Humphreys WG, Iyer RA and Li W (2015) Characterization of ADME properties of [^{14}C]asunaprevir (BMS-650032) in humans, Xenobiotica **46**:1-13.

Jana S and Paliwal J (2007) Molecular mechanisms of cytochrome p450 induction: potential for drug-drug interactions, Current protein & peptide science **8**:619-628.

Kosoglou T, Statkevich P, Johnson-Levonas AO, Paolini JF, Bergman AJ, Alton KB (2005) Ezetimibe: a review of its metabolism, pharmacokinetics and drug interactions, Clin Pharmacokinet 44:467–494.

LeCluyse E, Madan A, Hamilton G, Carroll K, DeHaan R and Parkinson A (2000) Expression and regulation of cytochrome P450 enzymes in primary cultures of human hepatocytes, Journal of biochemical and molecular toxicology **14**:177-188.

LeCluyse EL (2001) Human hepatocyte culture systems for the in vitro evaluation of cytochrome P450 expression and regulation, Eur J Pharm Sci 13:343-368.

Lutz JD and Isoherranen N (2012) In vitro-to-in vivo predictions of drug-drug interactions involving multiple reversible inhibitors, Expert Opin Drug Metab Toxicol 8:449-466.

Madan A, Graham RA, Carroll KM, Mudra DR, Burton LA, Krueger LA, Downey AD, Czerwinski M, Forster J, Ribadeneira MD, Gan LS, LeCluyse EL, Zech K, Robertson P Jr,Koch P, Antonian L, Wagner G, Yu L and Parkinson A (2003) Effects of prototypical microsomal enzyme inducers on cytochrome P450 expression in cultured human hepatocytes, Drug Metab Dispos **31**:421-431.

McPhee F, Sheaffer AK, Friborg J, Hernandez D, Falk P, Zhai G, Levine S, Chaniewski S, Yu F, Barry D, Chen C, Lee MS, Mosure K, Sun LQ, Sinz M, Meanwell NA, Colonno RJ, Knipe J and Scola P (2012) Preclinical Profile and Characterization of the Hepatitis C Virus NS3 Protease Inhibitor Asunaprevir (BMS-650032), Antimicrob Agents Chemother **56**:5387-5396.

Obach RS, Walsky RL and Venkatakrishnan K (2007) Mechanism-based inactivation of human cytochrome p450 enzymes and the prediction of drug-drug interactions, Drug Metab Dispos **35**:246-255.

Paris BL, Ogilvie BW, Scheinkoenig JA, Ndikum-Moffor F, Gibson R and Parkinson A (2009) In vitro inhibition and induction of human liver cytochrome p450 enzymes by milnacipran, Drug Metab Dispos **37**:2045-2054.

DMD #70409

Parkinson A, Kazmi F, Buckley DB, Yerino P, Ogilvie BW, Paris BL (2010) System-dependent outcomes during the evaluation of drug candidates as inhibitors of cytochrome P450 (CYP) and uridine diphosphate glucuronosyltransferase (UGT) enzymes: human hepatocytes versus liver microsomes versus recombinant enzymes, Drug Metab Pharmacokinet 25:16–27.

Robertson P, DeCory HH, Madan A and Parkinson A (2000) In vitro inhibition and induction of human hepatic cytochrome P450 enzymes by modafinil, Drug Metab Dispos **28**:664-671.

Scola PM, Sun LQ, Wang AX, Chen J, Sin N, Venables BL, Sit SY, Chen Y, Cocuzza A, Bilder DM, D'Andrea SV, Zheng B, Hewawasam P, Tu Y, Friborg J, Falk P, Hernandez D, Levine S, Chen C, Yu F, Sheaffer AK, Zhai G, Barry D, Knipe JO, Han YH, Schartman R, Donoso M, Mosure K, Sinz MW, Zvyaga T, Good AC, Rajamani R, Kish K, Tredup J, Klei HE, Gao Q, Mueller L, Colonno RJ, Grasela DM, Adams SP, Loy J, Levesque PC, Sun H, Shi H, Sun L, Warner W, Li D, Zhu J, Meanwell NA, McPhee F (2014) The discovery of asunaprevir (BMS-650032), an orally efficacious NS3 protease inhibitor for the treatment of hepatitis C virus infection. J Med Chem. 57:1730-1752.

Sims KD, Lemm J, Eley T, Liu M, Berglind A, Sherman D, Lawitz E, Vutikullird AB, Tebas P, Gao M, Pasquinelli C and Grasela DM (2014) Randomized, placebo-controlled, single-ascending-dose study of BMS-791325, a hepatitis C virus (HCV) NS5B polymerase inhibitor, in HCV genotype 1 infection, Antimicrob Agents Chemother **58**:3496-3503.

Sugiura N (1978) Further analysis of the data by Akaike's information criterion and the finite correction, Communications in Statistics **7**:13-26.

SUNVEPRA**®** [package insert] (2015). Bristol-Myers Squibb Australia Pty Ltd, Mulgrave, VIC, Australia. http://www.guildlink.com.au/gc/ws/bms/pi.cfm?product=bqpsunve10715

Tao X, Sims K, Chang Y-T, Rana J, Myers E, Wind-Rotolo M, Bhatnagar R, Xu T, Eley T, Garimella T, LaCreta F, AbuTarif M (2016) Effect of Daclatasvir/Asunaprevir/Beclabuvir in Fixed-dose Combination on the Pharmacokinetics of CYP450/ transporter Substrates in Healthy Subjects. 17th International Workshop on Clinical Pharmacology of HIV & Hepatitis Therapy. Washington, DC; June 2016

Tompkins LM and Wallace AD (2007) Mechanisms of cytochrome P450 induction, Journal of biochemical and molecular toxicology **21**:176-181.

US-FDA Draft Guidance (2008) Guidance for industry - Safety Testing of Drug Metabolites. http://www.fda.gov/Drugs/GuidanceComplianceRegulatoryInformation/Guidances/default.htm

US-FDA Draft Guidance (2012) Guidance for industry - Drug Interaction Studies – Study Design, Data Analysis, Implications for Dosing, and Labeling Recommendations. http://www.fda.gov/Drugs/GuidanceComplianceRegulatoryInformation/Guidances/default.htm

US-FDA Guidance (2013) Guidance for industry - M3(R2) Nonclinical Safety Studies for the Conduct of Human Clinical Trials and Marketing Authorization for Pharmaceuticals---Questions and Answers(R2). http://www.fda.gov/Drugs/GuidanceComplianceRegulatoryInformation/Guidances/default.htm

DMD #70409

Venkatakrishnan K, von Moltke LL, Obach RS and Greenblatt DJ (2003) Drug metabolism and drug interactions: application and clinical value of in vitro models, Current drug metabolism **4**:423-459.

Wilkins T, Malcolm JK, Raina D and Schade RR (2010) Hepatitis C: diagnosis and treatment, American family physician **81**:1351-1357.

Yao M, Zhu M, Sinz MW, Zhang H, Humphreys WG, Rodrigues AD, and Dai R (2007) Development and full validation of six inhibition assays for five major cytochrome P450 enzymes in human liver microsomes using an automated 96-well microplate incubation format and LC-MS/MS analysis, J Pharm Biomed Anal. **44**:211-223.

Zientek and Dalvie (2012) Use of a multistaged time-dependent inhibition assay to assess the impact of intestinal metabolism on drug-drug interaction potential, Drug Metab Dispos. 40(3):467-73.

Figure Legends

Figure 1   Chemical structures of Asunaprevir (ASV, BMS-650032), daclatasvir (DCV, BMS-790052), beclabuvir (BCV, BMS-791325), and BCV-M1 (major metabolite of BCV)

Figure 2   Curve fitting of CYP3A4 mRNA induction data from two individual donor hepatocytes treated with BCV using Simple E_{max} model and Four Parameter Logic model.

Figure 3   Strategies to evaluate CYP DDI risk for single and multiple perpetrators using static models

DMD #70409

Table 1. CYP3A4 mRNA change relative to DMSO (0.1%) treatment in hepatocytes from three human donors following incubation with ASV, DCV, BCV or BCV-M1.

Treatment		CYP3A4 mRNA[a]		
		Donor 1	Donor 2	Donor 3
ASV	Donor	HC3-15	HC1-18	HC5-10
	DMSO (0.1%)	1	1	1
	0.049 µg/mL	3.73[b]	nd	0.802
	0.15 µg/mL	1.53	1.86	1.13
	0.49 µg/mL	4.72	3.58	1.77
	1 µg/mL	7.79	5.5	2.92
	2 µg/mL	8.6	ND	3.66
	4.9 µg/mL	12.1	6.7	4.3
	10 µg/mL	8.7[c]	4.73[c]	3.7
	20 µg/mL	4.95[c]	2.39[c]	1.74[c]
	Rifampin (10 µM)	26	18.1	8.15
DCV	Donor	HC3-15	HC1-18	HC5-10
	DMSO (0.1%)	1	1	1
	0.16 µg/mL	1.38	1.45	1.21
	0.32 µg/mL	1.44	1.66	1.34
	0.75 µg/mL	2.5	2.27	1.47
	1.6 µg/mL	5.59	5.7	4.91
	2.5 µg/mL	7.48	9.22	3.7
	4 µg/mL	12.8	12.1	6.35
	6 µg/mL	20.3	13.2	6.68
	9.6 µg/mL	27.3	13	8.76
	Rifampin (10 µM)	26	18.1	8.15
BCV	Donor	HC3-15	HC3-17	HC5-10
	DMSO (0.1%)	1.00	1.00	1.00
	0.15 µg/mL	1.96	1.45	1.90
	0.35 µg/mL	3.27	1.99	1.67
	0.8 µg/mL	5.64	2.59	2.67
	1.5 µg/mL	6.36	2.61	2.43
	3.5 µg/mL	5.77	2.18	2.64
	8 µg/mL	3.88[c]	2.09	2.45
	15 µg/mL	2.70[c]	1.38[c]	1.43[c]
	30 µg/mL	0.29[c]	0.08[c]	0.26[c]
	Rifampin (10 µM)	29.80	3.70	7.93
BCV-M1	Donor	HC3-15	HC3-17	HC5-10
	DMSO (0.1%)	1.00	1.00	1.00
	0.028 µg/mL	1.04	1.15	0.97
	0.08 µg/mL	1.63	1.26	1.05
	0.28 µg/mL	3.57	1.99	1.61
	0.8 µg/mL	7.17	2.49	2.22
	2.8 µg/mL	8.23	2.26	2.41
	8 µg/mL	5.24[c]	2.14	1.89[c]
	15 µg/mL	3.78[c]	1.87[c]	3.08
	30 µg/mL	0.32[c]	0.15[c]	0.14[c]
	Rifampin (10 µM)	29.80	3.70	7.93

[a] Values are relative to vehicle control, normalized to GAPDH and are the average of triplicate determinations.

26

[b]. Anomalous data, possibly due to sample analysis error. Data were excluded from the curve fitting.

[c]. Data were excluded from the curve fitting as Fold Increase was <80% of the observed $E_{max.}$

Table 2 Induction kinetic parameters (E_{max} and EC_{50}) of ASV, DCV, BCV and BCV-M1following incubation with hepatocytes from three individual donors.

		Fold Induction			Fold Increase		
		HC3-15	HC1-18/HC3-17[a]	HC5-10	HC3-15	HC1-18/ HC3-17[a]	HC5-10
ASV	E_{max}	14.21	6.74	3.94	14.10	6.68	3.00
	EC_{50} (µg/mL)	1.00	0.61	0.58	1.38	0.68	0.78
DCV	E_{max}	28.24	13.05	8.27	45.30	11.90	12.80
	EC_{50} (µg/mL)	4.32	1.83	2.38	7.64	1.96	6.54
BCV	E_{max}	6.54	2.36	2.44	6.17	2.23	1.64
	EC_{50} (µg/mL)	0.20	0.03	0.02	0.46	0.45	0.19
BCV-M1	E_{max}	9.68	2.30	2.74	9.13	1.55	1.62
	EC_{50} (µg/mL)	0.39	0.02	0.21	0.58	0.19	0.47

[a], induction of ASV and DCV was evaluated using hepatocytes lot HC1-18; Induction of BCV and BCV-M1 was evaluated using hepatocytes lot HC3-17

28

Table 3 In vitro kinetic parameters of ASV, DCV, BCV and BCV-M1 interaction with human CYP3A4

	Reverse inhibition	TDI		Induction	
	$K_{i,u}$ (µg/mL)	K_{inact} (1/min)	$K_{I,u}$ (µg/ml)	E_{max}	EC_{50} (µg/ml)
ASV	2.72	0.032	1.035	7.93	0.95
DCV	1.91	ND	ND	23.33	5.38
BCV	2.62	ND	ND	3.35	0.37
BCV-M1	1.95	ND	ND	4.10	0.41

ND, not determined

29

Table 4 Summary of clinical studies and pharmacokinetic parameters

		Perpetrator drug				Midazolam oral dose (mg)	Reference
		Oral dose (mg)	Cmax (µg/mL)	f_u	k_a (min^{-1})	F_a	
ASV		200 BID	0.351	0.002	0.0063 [a]	1[b]	5	(Timothy Eley et al., 2011)
ASV		600 BID	0.632	0.002	0.0053 [a]	1[b]	5	(Unpublished data)[f]
DCV		60 QD	1.288	0.006	0.013 [a]	0.71	5	(M Bifano et al., 2013)
BCV		150 BID	1.835[c]/0.434[d]	0.012[c,d]	0.0067[a,c]	0.72[c]	5	(AbuTarif; et al., 2014)
BCV		300 BID	3.875[c]/0.944[d]	0.012[c,d]	0.0067[a,c]	0.72[c]	5	(AbuTarif; et al., 2014)
Triple I	ASV	200 BID	0.492	0.002	0.0063[e]	1	5	(Tao; et al., 2016)[g]
	DCV	30 BID	0.975	0.006	0.013[e]	0.71		
	BCV	75 BID	1.675[c]/0.350[d]	0.012[c,d]	0.0067[c,e]	0.72[c]		
Triple II	ASV	200 BID	0.473	0.002	0.0063[e]	1	5	(Tao; et al., 2016)[g]
	DCV	30 BID	0.974	0.006	0.013[e]	0.71		
	BCV	150 BID	3.141[c]/0.664[d]	0.012[c,d]	0.0067[c,e]	0.72[c]		

[a.] Determined based on plasma concentration profile from the same study

[b.] Fh of ASV is calculated to be 7%, lower than oral bioavailability of ASV (9.3%), suggesting ASV oral absorption is high in human. Thus Fa of ASV is set as 1.

[c.] values for BCV

[d,] values for BCV-M1

30

e. Determined based on plasma concentration profile from the single agent studies.

f. Data from an open-label, single-sequence study (AI447007), in which eighteen healthy subjects (17 male and 1 female) received: 1) a single oral dose of 5 mg midazolam on Day 1; 2) an oral dose of 600 mg ASV twice daily from Day 2 to Day 8; and 3) a single dose of 5 mg midazolam on Day 8 morning. The study protocol was approved by the Institutional Review Board at the investigational site. All subjects were closely monitored for adverse events throughout the study.

g. Data from an open-label, single-sequence study (AI443021), in which twenty healthy subjects (19 male and 1 female) received: 1) a cocktail of CYP and transporter probe substrates (including 5 mg midazolam) administered orally as a single dose on Day 1; 2) a combination of 200 mg ASV, 20 mg DCV, and 75 mg BCV administered orally twice daily from Day 6 to Day 20, and a cocktail of CYP and P-gp substrates (including 5 mg midazolam) administered orally as a single dose on Day 16; 3) a combination of 200 mg ASV, 20 mg DCV, and 150 mg BCV administered orally twice daily from Day 21 to Day 35, and a cocktail of CYP and transporter probe substrates (including 5 mg midazolam) administered orally as a single dose on Day 31. The study protocol was approved by the Institutional Review Board at the investigational site. All subjects were closely monitored for adverse events throughout the study.

31

Table 5 Predictions for clinical DDI studies using basic and mechanistic static model

Perpetrator drug	Observed AUC ratio (90% CI)	Predicted AUC ratio		
		R3 Average[a] (Individual[b])	AUCR Average[a] (Individual[b])	AUCR'[c] Average[a] (Individual[b])
ASV (200 mg BID)	0.71 (0.67-0.75)	0.32 (0.26; 0.31; 0.52)	2.36 (2.29; 2.37; 2.46)	0.50 (0.35; 0.54; 0.83)
ASV (600 mg BID)	0.56 (0.50-0.64)	0.24 (0.18; 0.24; 0.43)	3.02 (2.94; 3.01; 3.16)	0.70 (0.51; 0.75; 1.09)
DCV (60 mg QD	0.87 (0.83-0.92)	0.18 (0.13; 0.17; 0.32)	0.43 (0.33; 0.44; 0.68)	-
BCV (150 mg BID)	0.50 (0.45-0.57)	0.17 (0.10; 0.26; 0.31)	0.53 (0.34; 0.70; 0.72)	-
BCV (300 mg BID)	0.44 (0.40-0.48)	0.14 (0.08; 0.23; 0.27)	0.55 (0.34; 0.75; 0.77)	-
Triple Combination I (ASV: 200 mg BID; DCV: 30 mg BID; BCV: 75 mg BID)	0.53 (0.47-0.60)	0.084 (0.06; 0.17)	1.94 (1.70; 2.12)	0.33 (0.21; 0.59)
Triple Combination II (ASV: 200 mg BID; DCV: 30 mg BID; BCV: 150 mg BID)	0.42 (0.37-0.48)	0.078 (0.05; 0.16)	1.73 (1.45; 1.94)	0.32 (0.19; 0.58)

[a,] model prediction using the average values of EC_{50} and E_{max} from Table 3

[b], model prediction using the EC_{50} and E_{max} of individual donors from Table 2

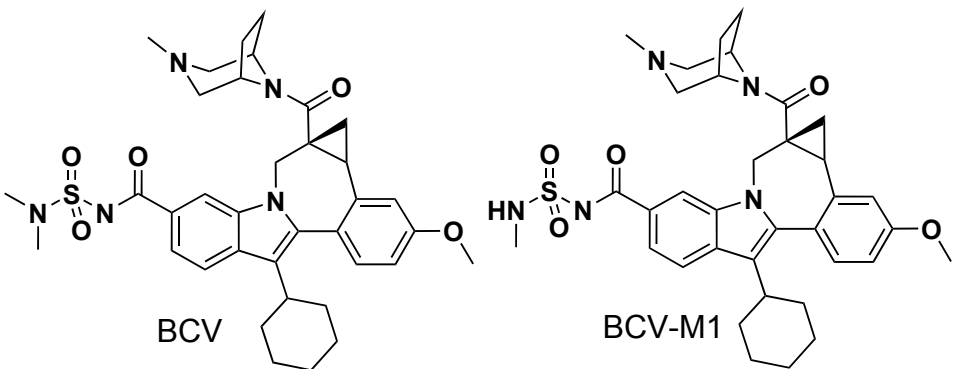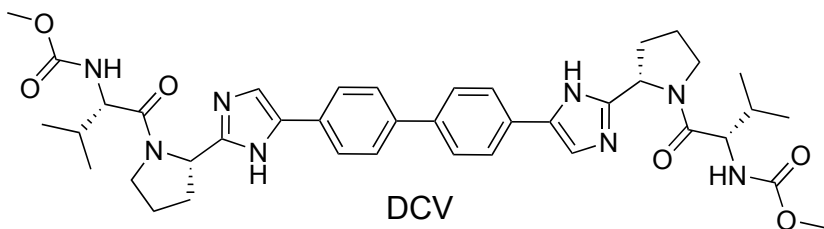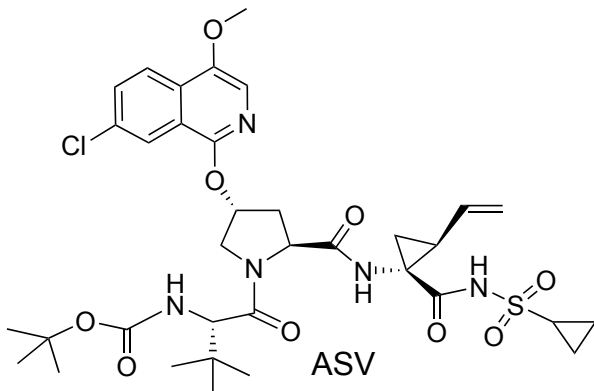[c], mechanistic static model approach not including the TDI effect of ASV
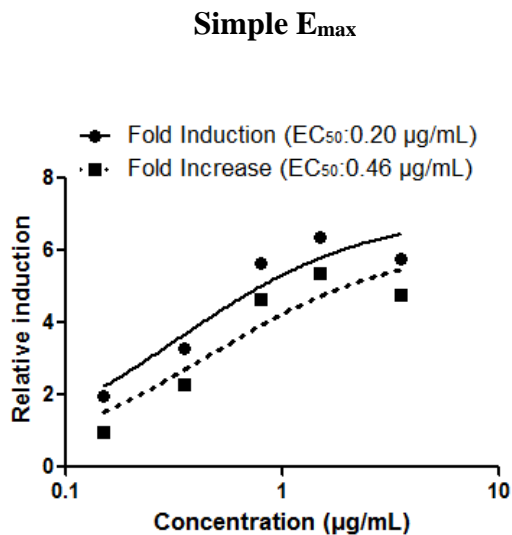
32

Figure 1

ASV
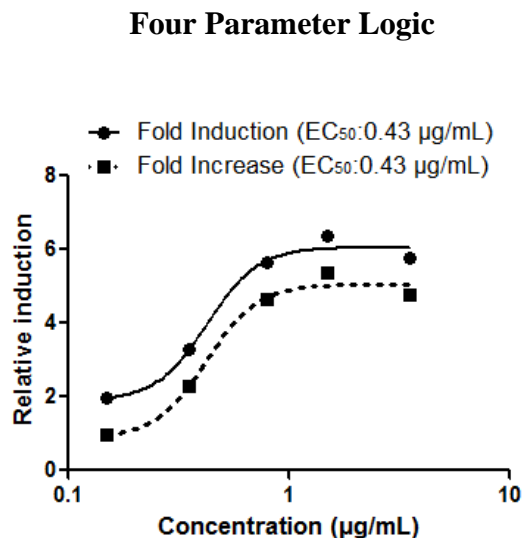
DCV

BCV

BCV-M1

Figure 2

Simple E$_{max}$

Four Parameter Logic

Donor 1

A

B

Donor 2

C

D

Figure 3